dc four-point resistance of a double-barrier quantum pump

Federico Foieri,[1] Liliana Arrachea,[1,2] and María José Sánchez[3]
[1]*Departamento de Física "J. J. Giambiagi" FCEyN, Universidad de Buenos Aires, Ciudad Universitaria Pab. I, 1428 Buenos Aires, Argentina*
[2]*BIFI, Universidad de Zaragoza, Pedro Cerbuna 12, 50009 Zaragoza, Spain*
[3]*Centro Atómico Bariloche and Instituto Balseiro, Bustillo 9500 8400 Bariloche, Argentina*
(Received 16 October 2008; revised manuscript received 30 December 2008; published 27 February 2009)

We investigate the behavior of the dc voltage drop in a periodically driven double-barrier structure (DBS) sensed by voltages probes that are weakly coupled to the system. We find that the four-terminal resistance R_{4t} measured with the probes located outside the DBS results identical to the resistance measured in the same structure under a stationary bias voltage difference between left and right reservoirs. This result valid beyond the adiabatic pumping regime can be taken as an indication of the universal character of R_{4t} as a measure of the resistive properties of a sample, irrespectively, of the mechanism used to induce the transport.

DOI: 10.1103/PhysRevB.79.085430 PACS number(s): 72.10.Bg, 73.23.−b, 73.63.Nm

I. INTRODUCTION

Quantum transport induced by time-dependent fields attracts presently an impressive amount of research. A phase-coherent conductor subjected to two periodically varying voltages becomes a paradigmatic example of a quantum pump, in which a dc current can be generated in the absence of a net external bias.[1–16]

After the works of Landauer and Buttiker,[17,18] the four-point resistance is considered as the proper measure of the genuine resistive behavior of a mesoscopic sample free from the effects of the contact resistance. Several theoretical works have been devoted to study the details of the voltage drop between the contacts in systems where the transport is induced by means of a stationary dc voltage bias.[19–22] Furthermore, the striking feature that resistance can be negative in a coherent conductor has been experimentally observed in semiconductors[23] and in carbon nanotubes.[24] However, the behavior of this physical quantity in the case of a quantum pump has not been so far analyzed. The aim of the present work is to investigate to what extent the concept of R_{4t} could depend on the underlying driving mechanism. To this end we investigate the dc four-terminal resistance for a quantum pump defined as the dc voltage drop $\Delta\mu_{PP'}$ sensed by the two probes, P, P' connected at two arbitrary points along the sample divided by the dc component of the current J^{dc} flowing through the device:

$$R_{4t} = \frac{\Delta\mu_{PP'}}{J^{\mathrm{dc}}}. \tag{1}$$

We will also compare this quantity with the four-terminal resistance obtained when the current through the device is induced by a slight stationary voltage difference between the reservoirs.

The paper is organized as follows. In Sec. II we present the model for the quantum pump, which mimics the actual double-barrier structure (DBS) used in the experiment of Ref. 1. The model Hamiltonian and the associated transport quantities obtained in the framework of the nonequilibrium Green's functions formalism are presented in this section. The analysis of the results is performed in Secs. III and IV. Section III is devoted to analyze the voltage profiles obtained analytically in the adiabatic pumping regime (which will be properly defined in this section) and to compare them with the numerical calculations. We compute the four-terminal resistance for the pumping setup which is compared with the same quantity obtained under stationary transport. In Sec. IV we extend the analysis beyond the adiabatic regime. Finally, Sec. V is devoted to the summary and conclusions.

II. THEORETICAL TREATMENT

A. Model Hamiltonian

We consider, as a model of the quantum pump, a quantum wire coupled to left and right reservoirs at a fixed chemical potential and with two narrow gates to which oscillating voltages are applied with a phase lag. This setup (see Fig. 1, upper plot) reproduces the actual DBS used in Ref. 1, where two of such ac potentials were applied at the walls confining a quantum dot. Experimentally, the dc response is actually inferred from the measurement of the voltage drop between two extra probes: one located at the left and the other at the

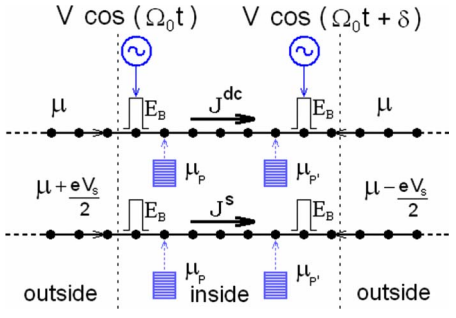

FIG. 1. (Color online) Scheme of the setup. The central device is a wire with two barriers of height E_B connected to L and R reservoirs. Two voltage probes P and P' sense the voltage drop. Upper plot: pumping setup in which a dc current J^{dc} is induced by two local ac voltages. The L and R reservoirs are at the same chemical potential μ. Lower plot: stationary setup, in which the current J^s is induced by a dc voltage difference V_s between L and R reservoirs. See text for more details.

right of the DBS. Accordingly, we consider noninvasive voltage probes weakly coupled to the wire.

The chemical potential μ_i $(i=P,P')$ of each probe is adjusted to maintain zero net current through the respective contact. We consider the simplest configuration, where the chemical potentials μ_P and $\mu_{P'}$ are purely dc. This simple model for the probes mimics a voltmeter which is able to *only* measure the dc voltage drop $\Delta\mu_{PP'}$. To compute the dc four-terminal resistance for the quantum pump defined in Eq. (1), we calculate below $\Delta\mu_{PP'}$ sensed by the two probes P,P', connected at two arbitrary points along the sample, and divide by the dc component of the current J^{dc} flowing through the device.

In addition, to compare with the four-terminal resistance computed under stationary transport, we will compute the current through the DBS induced by a slight stationary voltage difference V_s between the left (L) and right (R) reservoirs, as indicated in the lower panel of Fig. 1.

For the sake of clarity, we start considering just one voltage probe, which is modeled as a third reservoir coupled to the central system at the position P (the extension to more probes is trivial). The corresponding Hamiltonian for the full system reads as

$$H = H_{\mathrm{leads}} + H_P + H_C(t) - w_L(a_L^\dagger c_1 + \mathrm{H.c.}) - w_R(a_R^\dagger c_N + \mathrm{H.c.}) - w_P(a_P^\dagger c_p + \mathrm{H.c.}), \tag{2}$$

with $H_C(t)$ denoting the Hamiltonian for the central piece that we model as a one-dimensional (1D) tight-binding chain of length N with two barriers located at sites A and B,

$$H_C(t) = V\cos(\Omega_0 t + \delta)c_A^\dagger c_A + \sum_{l=1}^{N}\varepsilon_l c_l^\dagger c_l - w_h\sum_{l=1}^{N}(c_l^\dagger c_{l+1} + \mathrm{H.c.}) + V\cos(\Omega_0 t)c_B^\dagger c_B, \tag{3}$$

with w_h as the hopping parameter and the profile $\varepsilon_A=\varepsilon_B=E_b$ and $\varepsilon_l=0, l=1,\ldots,N\neq A,B$, defining a double-barrier structure. The time-dependent ac potentials act locally at the position of the barriers and have amplitude V and frequency Ω_0 and oscillate with a phase difference δ. We denote with H_{leads} the Hamiltonians of two semi-infinite tight-binding chains with hopping w_l at the same chemical potential μ, which play the role of the L and R reservoirs. These two leads are connected to the central device at sites $1,N$, respectively. Similarly, H_P is the Hamiltonian of the voltage probe P that we also model as a particle reservoir with a chemical potential μ_P that is fixed to satisfy the condition of net zero dc current through its contact to the central system.[18] The Hamiltonian of all the reservoirs may be written in a convenient basis as follows:

$$H_\alpha = \sum_{k_\alpha}\varepsilon_{k_\alpha}a_{k_\alpha}^\dagger a_{k_\alpha}, \tag{4}$$

where a_α are fermionic operators.

The contacts between the central system and the L and R leads and the probe P are described by the last three terms of Eq. (2), where the fermionic operators a_α $(\alpha=L,R,P)$. These operators are related to the fermionic operators a_{k_α} through a unitary transformation $a_\alpha=\Sigma_{k_\alpha}u_{k_\alpha}a_{k_\alpha}$, being $\Sigma_{k_\alpha}u_{k_\alpha}^2=1$.

B. General definition of the transport quantities

We employ the formalism of Keldysh nonequilibrium Green's functions, which is a convenient tool in transport theory on multiterminal structures driven by time-periodic fields. We briefly review the evaluation of the current through the contact between the central part and the reservoirs within this formalism and we defer the reader to previous literature for further details (see Refs. 15 and 16 and references therein). The time-dependent current (in units of e/h) through the contact between a given reservoir and the central system can be expressed in terms of the Green's functions as follows:

$$J_\alpha(t) = 2\sum_{k_\alpha} w_{k,\alpha}\,\mathrm{Re}[G^<_{l_\alpha,k_\alpha}(t,t)], \tag{5}$$

where $w_{k,\alpha}=u_{k,\alpha}w_\alpha$ and l_α denotes the site of the central system at which the reservoir $\alpha=L,R,P$ is attached, while we have introduced the lesser Green's function,

$$G^<_{l',l}(t',t) = i\langle c_l^\dagger(t)c_{l'}(t')\rangle. \tag{6}$$

The equation of motion of the lesser function (Dyson's equation) couples it to the retarded Green's function,

$$G^R_{l,l'}(t,t') = -i\Theta(t-t')\langle\{c_l(t),c_{l'}^\dagger(t)\}\rangle, \tag{7}$$

where $\{.,.\}$ denotes the anticommutator between the two operators. The corresponding equation in the present problem reads[2–13] as

$$G^<_{l,l'}(t,t') = \sum_\alpha\int_{-\infty}^{+\infty}dt_1dt_2G^R_{l,l_\alpha}(t,t_1)\times\Sigma^<_\alpha(t_1,t_2)\times[G^R_{l',l_\alpha}(t',t_2)]^*, \tag{8}$$

where we have introduced the "lesser" self-energy due to the coupling to the reservoirs

$$\Sigma^<_\alpha(t_1,t_2) = i\int_{-\infty}^{+\infty}\frac{d\omega}{2\pi}e^{-i\omega(t-t')}f_\alpha(\omega)\Gamma_\alpha(\omega), \tag{9}$$

being $f_\alpha(\omega)=1/(e^{\beta_\alpha(\omega-\mu_\alpha)}+1)$ as the Fermi function, which depends on the temperature and chemical potential of the reservoir α. In our calculations, we will consider the temperature $1/\beta_\alpha=0$. The function $\Gamma_\alpha(\omega)=|w_\alpha|^2\rho_\alpha(\omega)$ depends on the spectral function of the reservoirs $\rho_\alpha(\omega)=2\pi\Sigma_{k_\alpha}|u_{k_\alpha}|^2\delta(\omega-\varepsilon_{k_\alpha})$.

The evolution of the retarded Green's function is also given by the corresponding Dyson's equation. Due to the harmonic dependence in time of the Hamiltonian, it is convenient to use the following representation for the retarded Green's function:

$$G^R_{l,l'}(t,t') = \sum_{k=-\infty}^{\infty}\int_{-\infty}^{+\infty}\frac{d\omega}{2\pi}e^{-ik\Omega_0 t}e^{-i(t-t')}\mathcal{G}_{l,l'}(k,\omega), \tag{10}$$

which consists in a Fourier transformation with respect to the difference of times $t-t'$ and a Fourier expansion due to the periodicity in time that is equivalent to a Floquet expansion. Substituting Eq. (10) in Eq. (8) and the resulting expression in Eq. (5), after some algebra, the following expression is

obtained for the dc component of the current flowing through the contact to the reservoir α:

$$J_\alpha^{\rm dc} = \sum_{\beta=L,P,R} \sum_{k=-\infty}^{\infty} \int_{-\infty}^{\infty} \frac{d\omega}{2\pi} \{\Gamma_\beta(\omega)\Gamma_\alpha(\omega + k\Omega_0) \times |\mathcal{G}_{l_\alpha,l_\beta}(k,\omega)|^2 [f_\beta(\omega) - f_\alpha(\omega + k\Omega_0)]\}. \quad (11)$$

The voltage profile sensed by the probe can be exactly evaluated under general conditions from the solution μ_P that satisfies $J_P^{\rm dc}=0$ in the above expression with $\alpha=P$. In order to evaluate this exactly, we must exactly evaluate the retarded Green's function by solving the corresponding Dyson's equation,

$$G_{l,l'}^R(t,\omega) = G_{l,l'}^0(\omega) + \sum_{j=A,B} \sum_{k=\pm 1} e^{-ik\Omega_0 t} \times G_{l,j}^R(t,\omega + k\Omega_0) V_j(k) G_{j,l'}^0(\omega), \quad (12)$$

where $V_A(\pm 1) = Ve^{\mp i\delta}$ and $V_B(\pm 1) = V$. $G_{l,l'}^{0,R}(\omega)$ is the retarded Green's function of the system described by H [Eq. (2)] with $V=0$, i.e., in the absence of time-dependent fields and is the solution of the following set of linear equations:

$$G_{l,l'}^0(\omega)\left[\omega - \varepsilon_l - \sum_\alpha \delta_{l',l_\alpha} \Sigma_\alpha^R(\omega)\right] - \sum_{\delta=\pm 1} w_{l,l+\delta} G_{l,l'+\delta}^0(\omega) = \delta_{l,l'}, \quad (13)$$

where $w_{l,l+\delta}=w_h$ for $l \neq L,R$, while $w_{l,l+1}=0$ for $l=R$ and $w_{l,l-1}=0$ for $l=L$; while

$$\Sigma_\alpha^R(\omega) = \int_{-\infty}^{+\infty} \frac{d\omega'}{2\pi} \frac{\Gamma_\alpha(\omega')}{\omega - \omega' + i\eta} \quad (14)$$

is the retarded self-energy due to the coupling to the reservoir α.

III. ADIABATIC PUMPING REGIME: ANALYTICAL RESULTS

It is instructive to analyze first the case of low-driving frequency Ω_0 and small pumping amplitude V, which corresponds to the so-called adiabatic pumping regime.[2–13]

For low V, we can solve Eq. (12) by second-order perturbation theory in this parameter. It can be seen that the retarded Green's function contains only the following Floquet components that contribute to the dc current:[15,16]

$$\mathcal{G}_{l,l'}(\pm 1,\omega) \sim \frac{V}{2}[G_{l,A}^0(\omega \mp \Omega_0) G_{A,l'}^0(\omega) + e^{\pm i\delta} G_{l,B}^0(\omega \mp \Omega_0) G_{B,l'}^0(\omega)]. \quad (15)$$

As we already mentioned, we are considering "noninvasive probes." This corresponds to probes weakly coupled to the central system, in such a way that they do not introduce neither inelastic nor elastic-scattering process for the electronic propagation between L and R reservoirs. Under these conditions, from Eq. (11) we derive a general analytical expression for the voltage profile μ_P in the adiabatic regime,

$$\mu_P = \mu + \frac{\Omega}{\lambda}\left(\frac{V}{2}\right)^2 [|\mathcal{G}_{a,1}(1,\omega)|^2 + |\mathcal{G}_{a,N}(1,\omega)|^2 - |\mathcal{G}_{a,1}(-1,\omega)|^2 - |\mathcal{G}_{a,N}(-1,\omega)|^2], \quad (16)$$

where

$$\lambda = \sum_{k=0,1,-1} |\mathcal{G}_{a,1}(k,\omega)|^2 + |\mathcal{G}_{a,N}(k,\omega)|^2.$$

For weak coupling to the probes, Eq. (11) is evaluated with the Green's functions up to the first order in w_P. As $\Gamma_\alpha(\omega) \propto |w_\alpha|^2$, this corresponds to evaluate the functions $G_{l,l'}^0(\omega)$ from Eq. (13) with $\Sigma_P^R(\omega)=0$, i.e., the equilibrium retarded Green's functions of the central system attached only to the L and R reservoirs. We use these functions in Eq. (15). For perfect matching to the reservoirs ($w_L=w_R=w_l=w_h$) and for barriers with low amplitude $E_B \leq w_h$, these functions can be written in the following simple form:

$$G_{l,l'}^0(\omega) = g_{l,l'}(\theta) + E_B \sum_{j=A,B} g_{l,j}(\theta) g_{j,l'}(\theta), \quad (17)$$

with $g_{l,l'}(\theta) = ie^{-i|l-l'|\theta}/(2w_h \sin\theta)$ and $\omega = 2w_h \cos\theta$.[25] Using them to evaluate Eq. (15), substituting the result in Eq. (11), and considering the adiabatic ($\propto\Omega_0$) contribution in the resulting $J_P^{\rm dc}$, we get two different results depending on the place at which the probe is connected,

$$\mu_P = \mu \pm \Omega_0 V^2 \sin\delta[\alpha^o(k_F) + E_B\beta^o(k_F)], \quad x_P > x_B, \quad x_P < x_A,$$

$$\mu_P = \mu + \Omega_0 V^2 \sin\delta[\alpha^i(k_F,x_P) + E_B\beta^i(k_F,x_P)], \quad x_A < x_P < x_B, \quad (18)$$

with $x_j (j=A,B,P)$ denoting the position of the barriers and probe in units of the lattice parameter of the tight-binding model which we set to unit. The upper and lower signs of the first identity correspond, respectively, to the voltage probe located at the left ($x_P<x_A$) and right ($x_P>x_B$) sides of the DBS, while the second identity corresponds to the voltage probe located between the two barriers. We have defined the dimensionless Fermi vector (in units of the inverse of the lattice parameter) as $k_F \equiv \theta(\mu)$, as well as the following functions:

$$\alpha^o(k_F) = \frac{\sin[2k_F(x_A - x_B)]}{2(w_h \sin k_F)^2},$$

$$\beta^o(k_F) = \frac{\sin^2[k_F(x_A - x_B)]}{4(w_h \sin k_F)^3},$$

$$\alpha^i(k_F,x_P) = \sin[k_F(2x_P - x_A - x_B)]\alpha^o(k_F),$$

$$\beta^i(k_F,x_P) = \sin[k_F(2x_P - x_A - x_B)]\beta^o(k_F), \quad (19)$$

where the superscripts $o,(i)$ stress that the probe senses point outside (inside) the region where all the scattering processes (dynamical as well as stationary) take place.[26] In the simple model we are considering, with a perfect matching between the central system and the reservoirs, this coincides with the

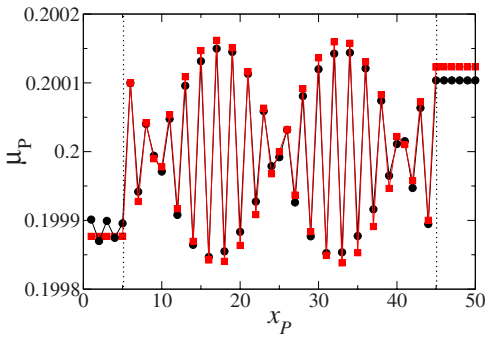

FIG. 2. (Color online) Local voltage μ_P sensed by the voltage probe P as a function of the probe position x_P along a DBS composed by $N=50$ sites with two barriers of height $E_B=0.2$ located at $x_A=5$ and $x_B=45$ as indicated by the vertical dashed lines. The pumping parameters are $V=0.01$, $\Omega_0=0.01$, and $\delta=\pi/2$. Red (dark gray) squares correspond to Eq. (18), the analytical solution for the adiabatic pumping regime, and a weakly connected probe. Black circles correspond to the exact numerical solution for the above pumping parameters obtained by equating Eq. (11) to zero with $w_P=0.01$. The chemical potential is $\mu=0.2$, which corresponds to $k_F=1.47$.

DBS, as indicated in Fig. 1. Equations (18) and (19) tell us that the local voltage sensed by a probe is constant outside the region defined by the DBS, while it presents the characteristic pattern of Friedel oscillations[19–22] with a period $2k_F$ at positions lying between the two oscillating barriers. Figure 2 shows the benchmark of the analytical result [Eq. (18)] against the exact voltage profile obtained numerically from Eq. (11) in the regime of weak V, Ω_0 and w_P, and a moderate E_B. A good agreement of the qualitative behavior is observed. In particular, the exact numerical profile μ_P exhibits Friedel oscillations with period $2k_F$ as a function of the probe position x_P as predicted by Eq. (18) and only a slight disagreement is found in the amplitude of the envelope function.

To the lowest order of perturbation in the coupling constant w_P, the effect of an additional second voltage probe P' is completely uncorrelated from the first one, since the associated interference effects involve second-order processes in w_P. At this level of approximation, let us call $\mu_{P'}$ as the local voltage sensed by the additional probe at P' and $\Delta\mu_{PP'} \equiv \mu_{P'}-\mu_P$ as the corresponding voltage drop. In a setup with the probe P (P') located at the left (right) side of the DBS, the voltage drop between both probes is from Eq. (18),

$$\Delta^o\mu_{PP'} = 2\Omega_0 V^2 \sin\delta[\alpha^o(k_F) + E_B\beta^o(k_F)]. \tag{20}$$

Another possible measurement corresponds to locate the voltage probes P and P' inside the DBS. In this case, the voltage drop between the two probes explicitly depends on the probe positions x_P and $x_{P'}$ as follows:

$$\Delta^i\mu_{PP'} = 2\Omega_0 V^2 \sin\delta\left\{\frac{\alpha^o(k_F) + E_B\beta^o(k_F)}{\sin[k_F(x_A - x_B)]}\right\} \times\cos\{k_F[(x_P - x_A) + (x_{P'} - x_B)]\}\sin[k_F(x_{P'} - x_P)], \tag{21}$$

where, as before, we have employed the superscripts $o,(i)$ to distinguish configurations with the probes outside (inside) the DBS.

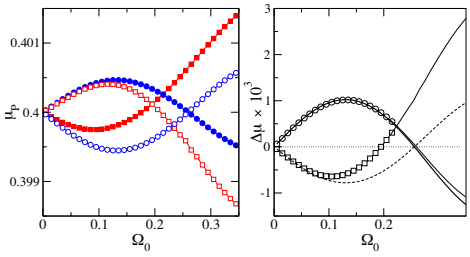

FIG. 3. (Color online) Left panel: local voltage profiles as a function of the pumping frequency Ω_0 obtained from the exact numerical calculation by equating Eq. (11) to zero. μ_P is sensed by a probe P located at $x_P=2$ (empty circles) or at $x_P=14$ (empty squares), respectively. The second probe P' senses the local voltage μ'_P at $x_{P'}=26$ (solid circles) or at $x_{P'}=38$ (solid squares). Notice that circles (squares) correspond to probes outside (inside) the DBS. Parameters are $\mu=0.4$, $N=40$, $E_B=0.2$, $x_A=10$, and $x_B=30$. Right panel: the corresponding potential drops $\Delta^{o,i}\mu_{PP'}$ computed for the above probes positions. Circles (squares) correspond to P and P' both located outside (inside) at sites $x_P=2$ and $x_P=38$ ($x_{P'}=14$ and $x_{P'}=26$) the DBS. The products $R_{4t}^{o,i}J^{\rm dc}$ (solid and dashed lines, respectively) between the exact current $J^{\rm dc}$ and the resistances evaluated from Eqs. (23) and (24), respectively. The vertical dotted line indicates the frequency of the pumping at which current inversion occurs.

Under the conditions assumed in the derivation of Eq. (18), i.e., low V, Ω_0, w_P, and E_B, the dc current flowing through the DBS reads as

$$J^{\rm dc} \cong 2\Gamma_L^0\Gamma_R^0\Omega_0 V^2 \sin\delta\left[\frac{\alpha^o(k_F) + E_B\beta^o(k_F)}{(2w_h \sin k_F)^2}\right], \tag{22}$$

with $\Gamma_\alpha^0 \equiv \Gamma_\alpha^0(\mu),(\alpha=L,R)$. We can now compute the dc four-terminal resistance R_{4t} in an adiabatic weakly driven pumping process. For a setup in which the probes are located outside the DBS ($x_P<x_A,x_B<x_{P'}$), it reads as

$$R_{4t}^o = \frac{\Delta^o\mu_{PP'}}{J^{\rm dc}} = \frac{(2w_h \sin k_F)^2}{\Gamma_L^0\Gamma_R^0}, \tag{23}$$

while it is

$$R_{4t}^i = \frac{\Delta^i\mu_{PP'}}{J^{\rm dc}} = E_B R_{4t}^o \frac{\sin[k_F(x_{P'} - x_P)]}{\sin[k_F(x_A - x_B)]} \times\cos[k_F(x_P - x_A + x_{P'} - x_B)], \tag{24}$$

for a setup in which the probes are located inside the DBS ($x_A<x_P<x_{P'}<x_B$).

We now turn to compare the value of R_{4t} obtained for the quantum pump with the resistance of the same DBS when the transport is induced through a stationary bias voltage V_s established by a difference in the electrochemical potentials of L and R reservoirs $\mu_L=\mu+eV_s/2$ and $\mu_R=\mu-eV_s/2$, as depicted in the lower panel of Fig. 1. Under the conditions of noninvasive probes and for linear response in V_s, it is possible to implement the same kind of perturbative procedure as before but for the stationary Green's functions. Assuming

again perfect matching between the DBS and the L and R reservoirs and $E_B < w_h$, we derive the following simple expression for the current flowing through the device:

$$J^s = \frac{\Gamma_L^0 \Gamma_R^0 V_s}{(2w_h \sin k_F)^2}, \tag{25}$$

which is the stationary counterpart of Eq. (22). From the above expression, we compute V_s/J^s and arrive immediately to the important identity,

$$R_{4t}^o \equiv \frac{V_s}{J^s}, \tag{26}$$

which tells that the dc four-point resistance measured in the quantum pump when the probes are connected outside the DBS R_{4t}^o [Eq. (23)] exactly coincides with the *total resistance* of the structure measured under stationary bias provided that the driving condition corresponds to the linear response in the stationary setup and the adiabatic regime in the pumping setup. At this point, it is important to recall that in the outside configuration the two probes enclose the whole region where all the scattering processes and, therefore, the full voltage drop V_s applied in the stationary setup takes place.

On the other hand, the counterpart of Eq. (24) for the stationary configuration reads as

$$R_{4t}^{s,i} \equiv R_{4t}^i \frac{\sin[k_F(x_A - x_B)]}{\sin k_F}, \tag{27}$$

which means that inside the DBS the dc resistance for the pumping setup differs from that under stationary driving just in a geometrical factor.

IV. BEYOND THE ADIABATIC REGIME: NUMERICAL RESULTS

Besides the relevance of the analytical results, it is valuable to analyze the response of the system beyond the adiabatic pumping condition. For that purpose, we have performed extensive numerical calculations of the dc current flowing through the system J^{dc} and the potential drop sensed by the voltage probes along the DBS, as a function of the pumping frequency Ω_0. In the left panel of Fig. 3, we plot the chemical potential μ_P as a function of Ω_0 for different locations of the probe x_P. In addition, in the right panel we have plotted the voltage drop $\Delta\mu = \mu_{P'} - \mu_P$ between two probes located outside the DBS (circles) and inside the DBS (squares).

When the frequency Ω_0 is close to the energy difference between two neighboring levels of the DBS, the latter becomes mixed by the pumping potential which causes an inversion in the sign of the dc current. A rough estimate for the frequency at which such a resonant condition is achieved in the example of Fig. 3 casts $\Omega_0 \sim 0.22$. In good agreement, we find an inversion in the sign of $\Delta^o \mu_{PP'}$ for probes connected outside the DBS at $\Omega_0 \sim 0.25$ (plots in circles of Fig. 3). Moreover, the voltage drop between two points outside the DBS in this case results identical to the product of the dc current J^{dc} times the value of the four-point resistance R_{4t}^o obtained in the adiabatic pumping regime in Eq. (23). In other words, our results indicate that even for pumping frequencies Ω_0 beyond the adiabatic regime, it is still possible to unambiguously define R_{4t}^o as the value obtained under the adiabatic approximation [Eq. (23)]. On the other hand, the voltage drop measured inside the DBS coincides with the product of R_{4t}^i times J^{dc} only within the adiabatic pumping regime, i.e., when $\Delta^i \mu_{PP'}$ depends linearly on Ω_0.

V. SUMMARY AND CONCLUSIONS

In this work we have computed the voltage profile and the four-terminal resistance in a DBS pumping setup. In the case of adiabatic pumping regime and for noninvasive voltage probes, we have obtained an analytical expression for the voltage profile across the DBS. We have shown that the four-terminal resistance R_{4t}^o measured in a pumping setup *for probes located outside the DBS* coincides with the total resistance of the structure measured under stationary bias. Our numerical results suggest that the result is valid also beyond the adiabatic regime. This can be taken as an indication of the universal character of R_{4t}^o as a concept to characterize the resistive properties of a system. However, this interesting possibility should be further investigated in other models with other ingredients such as disorder and many channels. It would be also interesting to generalize our model for the probes in order to consider the case where they are also affected by ac voltages.

ACKNOWLEDGMENTS

We acknowledge support from CONICET, PICT under Grant No. 0313829 (M.J.S.), and UBACYT (F.F. and L.A.), Argentina.

[1] M. Switkes, C. M. Marcus, K. Campman, and A. C. Gossard, Science **283**, 1905 (1999).
[2] L. DiCarlo, C. M. Marcus, and J. S. Harris, Jr., Phys. Rev. Lett. **91**, 246804 (2003).
[3] M. D. Blumenthal, B. Kaestner, L. Li, S. Giblin, T. Janssen, M. Pepper, D. Anderson, G. Jones, and D. Ritchie, Nat. Phys. **3**, 343 (2007).
[4] P. W. Brouwer, Phys. Rev. B **58**, R10135 (1998).
[5] I. L. Aleiner and A. V. Andreev, Phys. Rev. Lett. **81**, 1286 (1998).
[6] F. Zhou, B. Spivak, and B. Altshuler, Phys. Rev. Lett. **82**, 608 (1999).
[7] J. E. Avron, A. Elgart, G. M. Graf, and L. Sadun, Phys. Rev. Lett. **87**, 236601 (2001).
[8] V. Kashcheyevs, A. Aharony, and O. Entin-Wohlman, Phys. Rev. B **69**, 195301 (2004).

[9] J. Splettstoesser, M. Governale, J. Konig, and R. Fazio, Phys. Rev. Lett. **95**, 246803 (2005).
[10] S. Kim, K. K. Das, and A. Mizel, Phys. Rev. B **73**, 075308 (2006).
[11] E. Faizabadi, Phys. Rev. B **76**, 075307 (2007).
[12] V. Moldoveanu, V. Gudmundsson, and A. Manolescu, Phys. Rev. B **76**, 165308 (2007).
[13] A. Agarwal and Diptiman Sen, Phys. Rev. B **76**, 235316 (2007).
[14] M. Moskalets and M. Büttiker, Phys. Rev. B **66**, 205320 (2002); **69**, 205316 (2004); **78**, 035301 (2008).
[15] L. Arrachea, Phys. Rev. B **72**, 125349 (2005).
[16] L. Arrachea and M. Moskalets, Phys. Rev. B **74**, 245322 (2006).
[17] R. Landauer, Philos. Mag. **21**, 863 (1970).
[18] M. Büttiker, Phys. Lett. **57**, 1761 (1986); IBM J. Res. Dev. **32**, 317 (1988).
[19] J. L. D'Amato and H. M. Pastawski, Phys. Rev. B **41**, 7411 (1990).
[20] V. A. Gopar, M. Martinez, and P. A. Mello, Phys. Rev. B **50**, 2502 (1994).
[21] T. Gramespacher and M. Büttiker, Phys. Rev. B **56**, 13026 (1997).
[22] L. Arrachea, C. Naón, and M. Salvay, Phys. Rev. B **77**, 233105 (2008).
[23] R. de Picciotto, H. Stormer, L. Pfeiffer, K. Baldwin, and K. West, Nature (London) **411**, 51 (2001).
[24] B. Gao, Y. F. Chen, M. S. Fuhrer, D. C. Glattli, and A. Bachtold, Phys. Rev. Lett. **95**, 196802 (2005).
[25] F. Sols, M. Macucci, U. Ravaioli, and K. Hess, J. Appl. Phys. **66**, 3892 (1989).
[26] Notice that for the tight-binding model is meaningful only within the range $0<|k_F|<\pi$ (in the units we are working).